International Journal of Heat and Mass Transfer 101 (2016) 600–607

Contents lists available at ScienceDirect

International Journal of Heat and Mass Transfer

journal homepage: www.elsevier.com/locate/ijhmt

Optimization of a composite latent heat storage (CLHS) with non-uniform heat fluxes using a genetic algorithm

Henrik Veelken *, Gerhard Schmitz

Hamburg University of Technology, Institute of Thermo-Fluid Dynamics, Applied Thermodynamics, Germany

ARTICLE INFO

Article history:
Received 21 July 2015
Received in revised form 26 April 2016
Accepted 29 April 2016
Available online 4 June 2016

Keywords:
Phase change materials
Latent heat storages
Genetic algorithm
Optimization
Non-uniform heat fluxes
Effective heat capacity method

ABSTRACT

The scope of this work is to show optimization potential for regularly structured composite latent heat storage (CLHS) devices with non-uniform heat loads by varying the distribution of fins on the contact surface to an electronic component.

The modeling of the CLHS is carried out in 2D using Matlab in combination with Comsol and the effective heat capacity method for the melting process. The link between Matlab and Comsol is carried out with the Comsol–Matlab LiveLink. The modeled CLHS is a composite of aluminum with the phase change material (PCM) Parafol 22-95 (Sasol).

The optimization goal was the minimization of the surface-averaged temperature at the final time $t_f = 2400$ s on the contact surface. The optimization parameters were the positions of fins along this surface. Optimization results were compared to a CLHS with equally distributed fins and showed relative improvement of up to 3% for a certain aluminum/PCM-ratio.

The optimization was done using the genetic algorithm (GA) of Matlab on a high performance computer (HPC) at the Hamburg University of Technology (TUHH).

1. Motivation

In the field of power electronic cooling devices latent heat energy storage systems are a promising cooling system for time limited applications. The so called phase change materials have a benefit compared to other materials, since the melting enthalpy is many orders larger than the change in specific enthalpy due to a temperature rise of the same magnitude than the melting temperature range of materials not undergoing a phase change ($\Delta h_f \gg c\Delta T_m$). Because of their lower density and higher heat capacity, using PCMs instead of copper or aluminum reduces the weight and the volume of the heat storage significantly. Especially in aircraft applications this could be important. The drawback of these materials is a very low thermal conductivity. In order to improve the thermal conductivity of the heat storage device (HS), a material with high thermal conductivity, in this case an aluminum alloy ALSI12, has to be inserted such that the PCM is undergoing a uniform phase change from solid to liquid. The resulting system is called composite latent heat storage (CLHS) [1].

There are several publications about optimization of PCM-Systems. Most of them are concerning an entire energy system. Padovan and Manzan [2] have optimized a Solar Domestic Hot Water System using a genetic algorithm and the optimization tool modeFRONTIER. The modeling has been carried out using the code ESP-r. In their study they have shown, that the inclusion of PCM in the hot water tank does not improve the overall energy consumption of the system. An obvious parameter that does have impact on the overall energy consumption is the insulation thickness of the hot water tank.

Levin et al. [3] have carried out a numerical optimization of a PCM based electronic cooling device using a 2D-FEM Solver and a uniform boundary heat flux. The objective function they used is the sink operational time (SOT), which is the operating time, until a given set temperature T_{set} is reached. Usually T_{set} is the maximum operating temperature of the electric device. As one would expect, an energy storage device completely consisting of PCM or aluminum is worse than a CLHS. The main influencing parameters for SOT are number and length of fins, the heat flux at the interface between CLHS and electronic device and the difference between melting temperature T_m and T_{set}. Optimal PCM-percentages depend on the heat flux into the CLHS.

Nagose A [4] have also optimized PCM based electronic cooling devices using genetic algorithms. Discretizations were performed using the Finite-Volume method, which ensures energy conservation on a discrete level. The objective function used is

* Corresponding author.
E-mail addresses: Henrik.Veelken@tuhh.de (H. Veelken), Schmitz@tuhh.de (G. Schmitz).

http://dx.doi.org/10.1016/j.ijheatmasstransfer.2016.04.121
0017-9310/

Nomenclature

Δh_f	specific melting enthalpy [kJ/kg]
ΔT_m	melting temperature range [K]
$\Gamma_{1,t}$	$\Gamma_1 \times [0, t_f]$ [m^2 s]
Γ_1	adiabatic outer surface (see Fig. 2) [m^2]
$\Gamma_{2,t}$	$\Gamma_2 \times [0, t_f]$ [m^2 s]
Γ_2	outer surface with inward heat flux [m^3 s]
Γ_c	surface between foil and CLHS [m^2]
Ω_s	volume occupied by the CLHS [m^3]
Ω_t	$\Omega_s \times [0, t_f]$ [m^3 s]
$\overline{T}_{e-s,V}$	mean temperature in Ω_s for equal spaced fins [K]
$\overline{T}_{o-s,V}$	mean temperature in Ω_s for optimal spaced fins [K]
ρ	density [kg/m^3]
ε	minimal distance between two starting points (x_i) [m]
c	specific heat capacity [kJ/(kg K)]
J	objective function (see (9)) [K]
k	thermal conductivity [W/(mK)]
n	number of fins
$n_{1/2}$	outer normal vector on $\Gamma_{1/2,t}$
$r_i(\tau)$	curve, which is perpendicular to time-averaged temperature field resulting from pure PCM in the CLHS
$s(x,y)$	function defined in Ω_s, which represents the fins ($(s=1) \hat{=}$ aluminum, $(s=0) \hat{=} PCM$)
T_0	temperature at $t = 0$ s [K]
t_f	final time [s]
x_i	starting points for curves r_i, optimization parameters [m], (see (11))
ANN	artificial neural network
CLHS	composite latent heat storage
GA	genetic algorithm
OP	optimization program
PCM	phase change material
SOT	sink operational time

$f = SOT^{0.7}\alpha_{set}^{1.4}$, where α_{set} is the percentage of melted PCM at the time, when T_{set} is reached. As it can be seen from their work optimizing SOT and α_{set} does not lead to the same optimal parameter set. Levin et al. [3] has argued, the reason for this might be, that the PCM-material has a range of temperatures, at which a phase change occurs at constant pressure. Therefore it might be preferable to have PCM-material which is in the process of melting at the time T_{set} is reached. Nagose A [4] have published a correlation for an optimal heat spreader thickness δ and percentage of PCM φ for a given height A of the CLHS.

Baby and Balaji [5] have carried out experimental investigations on the cooling performance of pin-fin, plate-fin and no-fin CLHS. They have shown, that the enhancement ratio (SOT of pin/plate-fin over no-fin CLHS) of pin-fin type CLHS is between 32% and 134% larger than of plate-fin type CLHS. In a second study Baby and Balaji [6] have carried out experimental investigations with different numbers of pin fins. These experiments were used to train an artificial neural network (ANN). The ANN was then used to optimize the SOT using a genetic algorithm. It should be mentioned though, that ANNs are only capable of predicting outputs of system, which are in a close environment of the trained data. Therefore predicting the output for non-uniform heat loads would include large uncertainties. Baby and Balaji [6] have reported, that convection within the melted PCM is the main reason for a uniform temperature distribution within the PCM in pin-finned CLHS and suggested to include convection in PCM-melting simulations.

Lohse [7] has proposed a promising strategy for the design of structures in CLHS with non-uniform heat fluxes: first simulate a CLHS with only PCM, following an insertion of fins, which are aligned to the time-averaged gradient of the temperature field. The optimal distribution for such fins has not been studied yet. This was carried out in this work.

2. Basic simulation model

To simulate the phase change process a 2D-FEM simulation model in COMSOL Multiphysics is used. In the following chapters surface is used for a line and volume for an area in the 2D-model. The parameters of the model are the same as in Lohse and Schmitz [1] and can therefore be seen as validated. The equation that is solved within the CLHS is the following heat equation

$$\rho(s)c(s,T)\frac{\partial T(x,t)}{\partial t} - \nabla \cdot k(s)\nabla T(x,t) = 0 \text{ in } \Omega_t = \Omega_s \times [0, t_f] \quad (1)$$

$$k(s)\frac{\partial T(x,t)}{\partial n_1} = 0 \text{ on } \Gamma_{1,t} \quad (2)$$

$$k(s)\frac{\partial T(x,t)}{\partial n_2} = \dot{q} \text{ on } \Gamma_{2,t} = \partial\Omega_t \setminus \Gamma_{1,t} \quad (3)$$

$$T(x,0) = T_0(x) \text{ in } \Omega_s \quad (4)$$

$$\rho(s) = s \cdot \rho_{Alu} + (1-s) \cdot \rho_{PCM} \quad (5)$$

$$k(s) = s \cdot k_{Alu} + (1-s) \cdot k_{PCM} \quad (6)$$

$$c(s,T) = s \cdot c_{Alu} + (1-s) \cdot \left(c_{PCM} + \Delta h_f \frac{c_b e^{-c_b(T-T_m)}}{(1+e^{-c_b(T-T_f)})^2} \right) \quad (7)$$

with parameters given in Table 1 and s a function representing the fins and defined in $\Omega_s = [-0.05m, 0.05m]^2$ which takes values in $[0,1]$. A heat equation with constant material properties is solved outside the CLHS.

In Fig. 1 $s(x,y)$ is plotted for $(x,y) \in \Omega_s$, black symbolizes aluminum (i.e. $s = 1$) and white PCM (i.e. $s = 0$). The field s is stored in a matrix defined on a Cartesian grid with gridsize 200 μm. The following topology optimization program can be adopted to many different optimization programs, like fin thickness, varying fin thickness along one fin etc. Values for s have to be imported into COMSOL, since the description of s is a MATLAB function. For this task the MATLAB LiveLink is used. For values of $(x,y) \in \Omega_s$, which lie in between the Cartesian grid points, $s(x,y)$ is linearly interpolated. The grid for the simulation in Comsol is the same than the Cartesian grid in MATLAB, therefore the discrete temperature field T is defined on the same points than s inside the CLHS. A detailed view of the mesh can be seen in Fig. 2 on the right side. On the left side the simulation setup can be seen where in the upper part the s-controlled CLHS is shown, below a thermally conductive foil with $k = 6.5$ WK/m and a copper construction, which is a 2D-representation of heated stripes (see Fig. 3, RHS). In between the

Table 1
Constants heat equation.

$k_{PCM} = 0.162$ W/(mK)	$k_{Alu} = 160$ W/(mK)	$\Delta h_f = 250$ kJ/kg
$\rho_{PCM} = 780$ kg/m^3	$\rho_{Alu} = 2700$ kg/m^3	$T_m = 41.6\,^\circ C$
$c_{PCM} = 3.3$ kJ/(kg K)	$c_{Alu} = 0.9$ kJ/(kg K)	$c_b = 1.3$

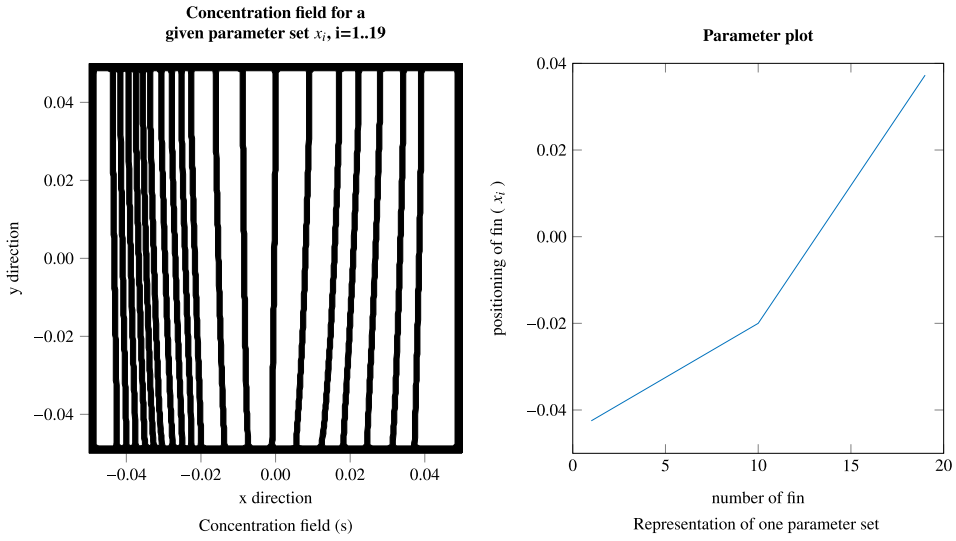

Fig. 1. Concentration field (s) and parameter visualization.

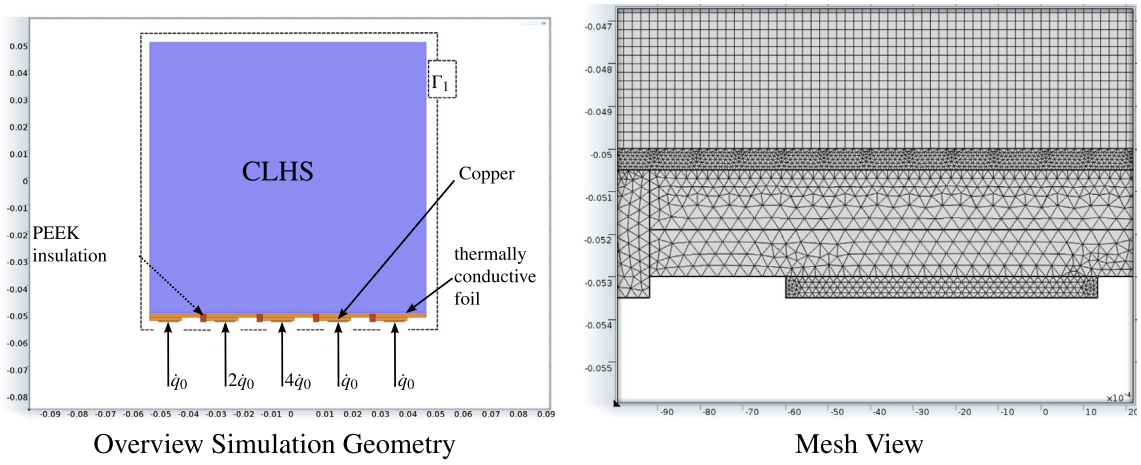

Fig. 2. Overview model setup.

Fig. 3. Image of heated stripes with copper plates and power resistor.

heated stripes a thermoplastic Polyether ether ketone (PEEK) insulation block is modeled, in order to thermally isolate the heated stripes with different heat loads. PEEK is both mechanically stable and easy to mill. On the LHS of Fig. 3 one can see a CLHS, the heated copper stripes and the PEEK plate.

In the current work the heat load $\dot{q}$ is one of the following $\dot{q}_0, 2\dot{q}_0, 4\dot{q}_0$, where $\dot{q}_0 = 13661.2\,\mathrm{W/m^2}$. Since most of the power electronic equipment does not have a spatially constant distribution of waste heat, the heat loads are chosen to be non-uniform. The peak heat waste in aircraft applications is about $170,000\,\mathrm{W/m^2}$. The averaged heat load in this work is $9000\,\mathrm{W/m^2}$, which is about 20 times smaller, since smaller heat loads are easier to be realized in subsequent experiments. The heat flux is imposed on the lowest surface of the heated stripes. On Γ_1, the outer surface without an imposed heat flux, adiabatic boundary conditions are set.

Simulation times for a single evaluation in this study is around one hour on 4 cores. Simulations including convection would result in simulation times, which are much larger and could not be used

for optimization programs anymore. Since the paper is focused on the optimization we neglected convection, which is considered to be non-significant because of the narrow space between neighboring fins.

3. Optimization setup

While Lohse and Schmitz [1] claimed that the main parameters for a CLHS assessment are temperature homogeneity, temperature rise during phase change and the ratio of melting time and melting time of an ideal CLHS a different approach is taken in this work. It is assumed that the Volume, that the CLHS occupies, is fixed and an optimal distribution of aluminum and PCM in the CLHS has to be found. Srinivas and Ananthasuresh [8] has suggested to use the objective function

$$J(t,s) = \|T(s) - T_0\|^2_{L_2(\Gamma)} = \int_\Gamma (T(s) - T_0)^2 \, dA \tag{8}$$

where T is the time depended temperature, T_0 is the temperature at the beginning of the simulation and Γ is the contact surface with the inward heat flux. The L_1-Norm is chosen in this work as an objective function, since it has a direct physical interpretation, which is the temperature increase averaged over the surface Γ. As the heat flux is not directly connected to the controlled space, the surface at which the objective function is evaluated is the surface at the top of the conductive foil. In this study the objective function is evaluated at the final time ($t = t_f$). Therefore the objective function in this study reads

$$\begin{aligned} J(t = t_f, s) &= \frac{1}{|\Gamma_c|} \|T(s) - T_0\|_{L_1(\Gamma_c)} \\ &= \frac{1}{|\Gamma_c|} \int_{\Gamma_c} |T(s) - T_0| \, dA \end{aligned} \tag{9}$$

Since the inward heat flux is constant in time the temperature at every point is strictly monotonically increasing. Therefore the absolute value can be omitted and while using J as objective function, not only the spatially-averaged temperature increase is minimized but also the maximum of the spatially-averaged temperature increase with respect to time (see Fig. 9).

$$\max_{t \in [0, t_f]} J(t,s) = J(t = t_f, s)$$

In order to follow the procedure proposed by Lohse [7], first a temperature field is calculated using purely PCM, i.e. $s(x) = 0, \ \forall x \in \Omega_s$. This temperature field is averaged over time $\overline{T}$ and fins are inserted perpendicular to isothermal surfaces. Mathematically the ODE

$$r_i'(\tau) = -\nabla \overline{T}(r_i(\tau)) \tag{10}$$

$$r(0) = x_i \tag{11}$$

has to be solved. x_i is the starting point of fin i at the contact surface. Note that the gradient of a field variable is always perpendicular to its isosurfaces. Here τ is a curve parameter and $r_i(\tau)$ is a curve point in Ω_s. This ODE can be computed using the ODE-Toolbox from Matlab. The solution can be seen in Fig. 4. The control field s (Fig. 1) is now created by calculating the minimal distance of a grid point to a set of curves. If this distance is less than half the diameter of a fin (in this study 1.4 mm), s is set to 1 at this point, else it is set to 0. In Fig. 4 the spatial positioning of the fins at the contact surface (x_i-values) is equally spaced with 19 fins. It turns out, that the fins are spread above the hot spots in the middle. Therefore the fins should be concentrated above hot spots. In the following chapter an optimal parameter set of x-positions of the fins is computed, i.e. an optimal parameter set for x_i is sought.

Therefore the optimization program is the following

$$\min_{x_i \in [-0.05, 0.05], i = 1 \ldots n} J(t = t_f, s(x_1 \ldots x_n)) =: \widetilde{J}(x_1 \ldots x_n), \tag{12}$$

where n is the number of fins. The search space can be reduced, if one uses the symmetric property of $\widetilde{J}$ (numbering of the fins is arbitrary). The following linear constrained is added

$$x_i \leqslant x_{i+1} - \varepsilon, \quad i = 1, \ldots, n \tag{13}$$

where ε is an arbitrary positive number (in this study $\varepsilon = 1$ mm). This linear constraint ensures, that the number of the fins is from left to right and a minimum distance exist between all fins.

4. Optimization procedure

In order to find an optimal parameter set for the optimization program (OP) (12) and (13) a GA is used. As described in many different papers the GA is a heuristic procedure to find a global optimum of OP. At each iteration (generation) a so called population is evaluated. To create a new population for the next generation the fittest individuals (one parameter set) are directly transferred (elitism), an average of two individuals is taken (crossover) or an individual is randomly changed (mutation). With growing iterations a lower value for the objective function is sought.

Some of the advantages of the GA are

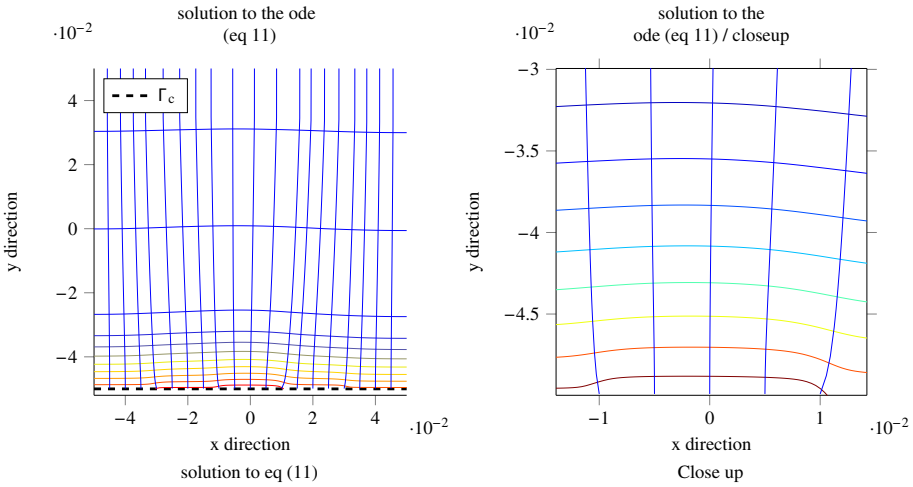

Fig. 4. Contour lines of the time-averaged temperature field and fins which are perpendicular aligned to it.

- Good parallelization possibilities, since the individuals within one population don't depend on each other.
- Only the objective function at a given parameter set has to be evaluated. This is very useful for OPs with an objective function that is subject to noise, as in PDE-based OPs.
- The GA does not necessarily converge at a local minimum.

Where some of the drawbacks are

- A lot of computational power is needed to calculate an optimal parameter set.
- The GA is not a deterministic algorithm and there is no guarantee, that even though the GA converges at a parameter set, this set is even a local minimum.

As the objective function for this OP cannot be calculated exactly and is subject to noise the derivative cannot be calculated numerically well enough to find an optimal parameter set. Tests have shown, that even if the number of fins is small (less than 5), a gradient based optimization algorithm stops after few iterations with an optimal parameter set, which is obviously non-optimal.

The calculation of the first randomly chosen population has been changed, since the variability of the first population calculated by a default Matlab function is very low. The main reason for this must be seen in the linear constraints, since dropping these constraints will lead to better variability in the first population. The algorithm can be seen in Algorithm 1. Since the linear constraints (13) have to be fulfilled, the sum of distances between two neighboring fins Δ or the boundary is set to the total length minus $n+1$ times the minimal distance between two fins (ε). Now a random portion of Δ is subtracted from it, stored in δ_i and repeated for all fins. Taking $x_i = x_{i-1} + \varepsilon + \delta_i$ would result in larger gaps between fins on the left side of the CLHS. Therefore for each gap a random number is taken from $\delta_{1..n}$. A starting population has to have m individuals, therefore this calculation is repeated for m times.

Algorithm 1. Calculation of initial population (pseudo code)

$n \leftarrow \#fins$
$m \leftarrow \#individuals$
for k=1:m **do**
  $\Delta \leftarrow 0.05 \cdot 2 - (n+1) \cdot \varepsilon$
  for i=1:n+1 **do**
    $\delta_i \leftarrow \Delta \cdot randomReal_{[0..1]}$
    $\Delta \leftarrow \Delta - \delta_i$
    if $\Delta < 0$ **then**
      $\Delta \leftarrow 0$
    end if
  end for
  $x_1 \leftarrow -0.05$
  for i=2:n+1 **do**
    $j \leftarrow randomInteger(length(\delta))$
    $x_i \leftarrow x_{i-1} + \varepsilon + \delta_j$
    $\delta \leftarrow \delta_{1,..j-1,j+1,..,end}$
  end for
  $x \leftarrow x_{2:end}$
  $initPop_{k,1..n} \leftarrow x$
end for

A population plot of the first generation is plotted in Fig. 5. It turns out the diversity of the first population is quite large. As the optimal distribution of fins is close to an equally spaced distribution, a better initial population might be one, that is created from an equally spaced distribution plus a small random change of the positions x_i, which is smaller than half of the spacing between two fins. In case one computes a new optimal distribution for a different heat load, this approach might lead to a faster converging algorithm. An optimization run with a differing initial population has not lead to a speed up of the algorithm. In fact, the algorithm was around 75% slower compared to an optimization run with an initial population given by Algorithm 1.

It should be mentioned, that most of the time spent on this optimization program was needed to efficiently calculate different individuals in parallel on different nodes, while handling issues like licensing, crashes with a broken environment for Comsol and automatically recomputing crashed function evaluations.

For this study a new hardware environment of the Technical University of Hamburg-Harburg was used. The nodes used for this calculation consisted of two Intel E5-2680v3-Cores with either 128 GB or 256 GB of memory. Each node has therefore 24 cores, so a large computational time can be saved by using say 2 nodes with jobs that use 2 cores. The programming for the parallel execution was carried out in bash (Unix-shell) and Matlab.

5. Results

In this section the optimization results are discussed. In Fig. 5 the population is plotted for different generations of the GA. The optimal distribution at each generation is highlighted as well as an evenly spread distribution. The number of fins is set to 19. One can clearly see the contraction of the generation towards the optimal value, which can be seen in the bottom right plot. Higher lines represent individuals with fins placed rather on the right, while lower lines represent individuals with fins placed rather on the left. As expected, lines, that are placed on the higher or lower end of the first population, are eliminated rapidly from the population, but might still be necessary to keep a large diversity in the population and for the creation of "good" crossovers.

The optimal distribution is from fins 1–10 above and subsequently from 11–19 below the equally spaced curve. Further one can observe, that the slope of the distribution is decreasing towards the 11th fin continued by an increase, such that the equally distributed line is approached. Looking at the ordinate, one observes, that the 12th fin is the last fin which is inside the high heat load area. So the results show the behavior, which might have been expected, that the fins are concentrated around the higher heat load areas.

Most of the individuals of the last generation have fins, which are positioned to the right of the optimal distribution (the graph of the optimal distribution lies at the lower end the population). Therefore the GA is very slowly approaching an optimal distribution at higher generations.

The objective function J for the fittest individual for each generation can be seen in Fig. 6 on the left side. One can clearly see, how it drops from iteration 1 to around 30. After iteration 30 the GA converged to a state, where a measurable decrease is not achieved anymore.

On the right side of Fig. 6 one can see a comparison between the optimal distribution objective function and the objective function achieved by an equally spaced distribution for different mesh resolutions. The optimal value approaches a minimal value near 19 fins. An explanation for this behavior might be, that the fin thickness is chosen in such a way, that for 19 fins the volumetric concentration of aluminum is close to 30%. As the fin thickness is constant for all optimization cases, the volumetric concentration

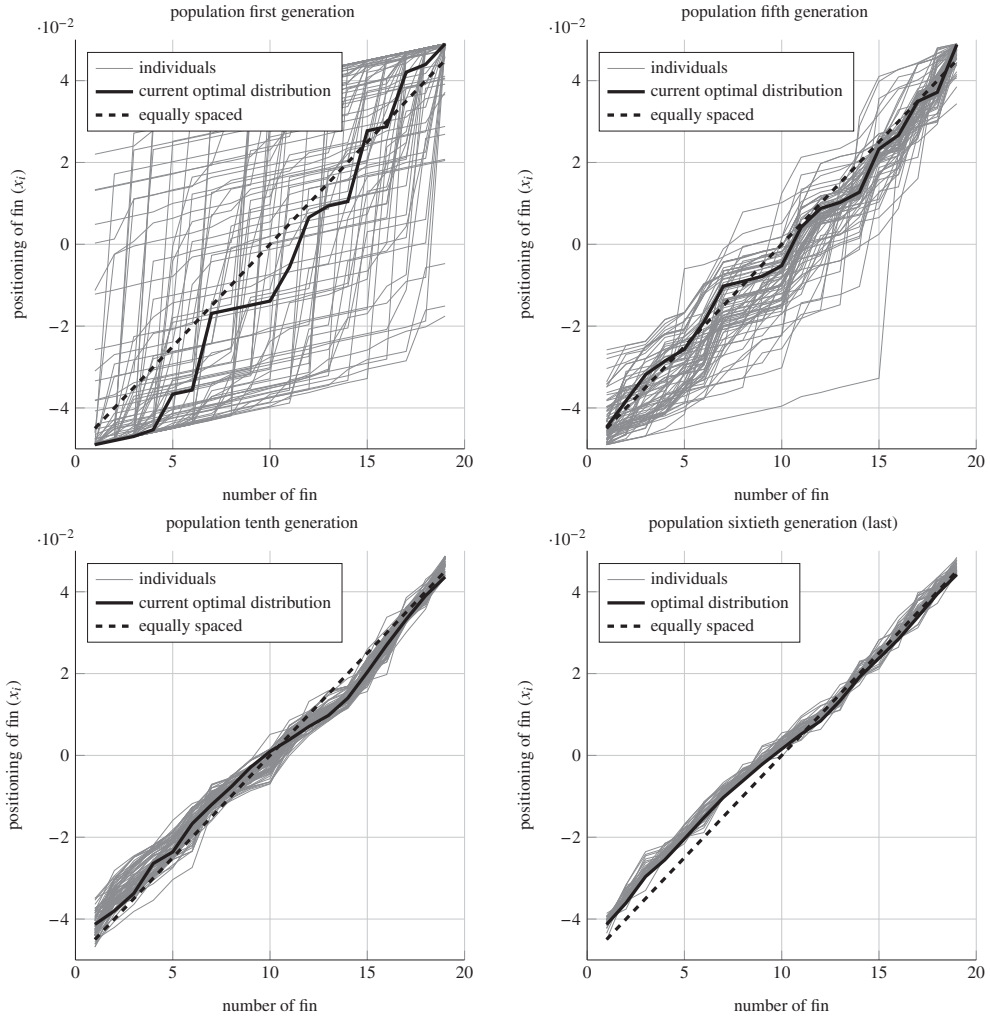

Fig. 5. Population at different stages of the optimization program, 19 fins (values for optimal distribution see Table 3).

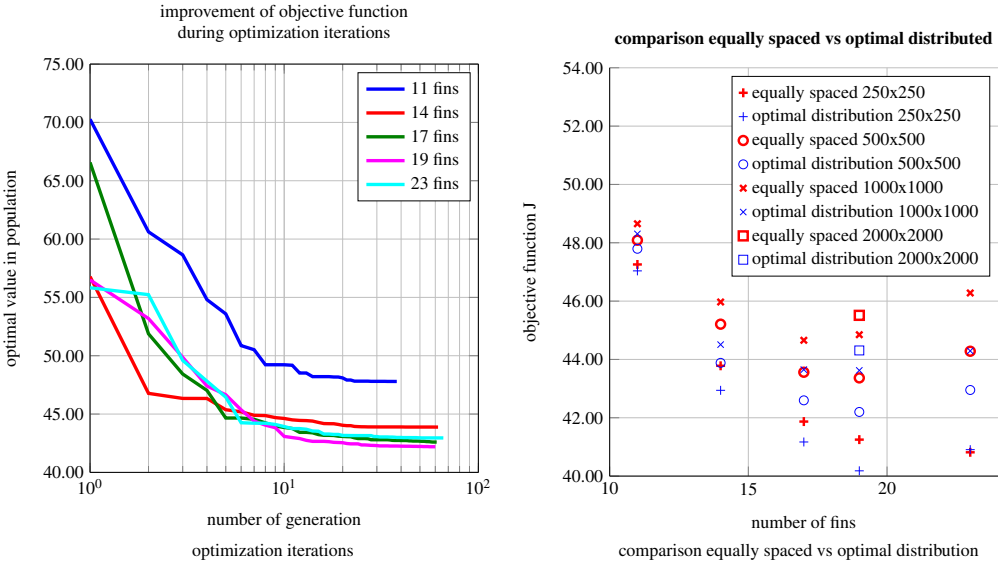

Fig. 6. Optimization iterations and optimal results comparison.

changes with the number of fins inserted into the CLHS. Therefore 30% volumetric concentration might be seen as the optimal value for this setup.

With increasing mesh resolution the spatially averaged temperature is increasing while the change between two meshes is decreasing. A mesh refinement only in the Comsol simulation (the mesh for

$s(x, y)$ has not been changed) has shown, that the spatially averaged temperature increase is due to a better mapping of the fin geometry. For the mesh resolutions 500×500, 1000×1000 and 2000×2000 the difference between o−s and e−s distributions is almost constant except for the optimization case with 23 fins. Simulation times for the 1000×1000 mesh were around 10.5 hours and for the 2000×2000 mesh around 98 h on 12 cores. In summary the mesh resolution of 500×500 is sufficient.

It turns out, that a change in the distribution of the fins will lead to an improved result and should therefore be considered during the development of a CLHS. The relative improvement for 19 fins is about 2.8%. The main reason for this improvement can be seen in Fig. 7. In this image the liquid fraction is shown at the final time t_f. A value slightly above 0 marks the beginning of the melting process while a value slightly below 1 marks the end of the melting process. Because of the spreading of fins above the hot spot the melting process is not finished in this area (see left image), while with an optimal spaced distribution the lowest value for the liquid fraction is about 0.9, therefore the melting process is almost finished. With an equally spaced distribution some of the latent heat capacity is not used which leads to a higher temperature at $t = t_f$.

In Fig. 8 the temperature as well as the temperature against the mean temperature in the CLHS ($\overline{T}_{e-s,V}, \overline{T}_{o-s,V}$) is plotted at the contact surface for $t = t_f$. One can see, that the shape of the temperature plot is for both cases (e−s = "equally spaced", o−s = "optimal spaced") quite the same. The difference is a shift of at least 1 K up to 2 K. Therefore the maximum temperature that the electronic component exhibits is also reduced by the same amount than $\widetilde{J}$ is.

In order to compare T with $\overline{T}_{e-s/o-s,V}$ the L_1 and L of the difference is computed:

$$\begin{aligned}
\|T - \overline{T}_{e-s,V}\|_{L^1(\Omega_s)} &= 4\ \text{K} \\
\|T - \overline{T}_{e-s,V}\|_{L^\infty(\Omega_s)} &= 14.37\ \text{K} \\
\|T - \overline{T}_{o-s,V}\|_{L^1(\Omega_s)} &= 3.4\ \text{K} \\
\|T - \overline{T}_{o-s,V}\|_{L^\infty(\Omega_s)} &= 12.21\ \text{K}
\end{aligned} \tag{14}$$

The maximum deviation from the averaged temperature is therefore not exhibited at Γ_c (see Fig. 8) and the temperature distribution is more uniform in the optimized case.

Table 2 in the appendix shows the equivalent to Fig. 8 for each optimization case at given x-positions. Optimal parameters for all of the optimization cases can also be seen in the appendix (Table 3).

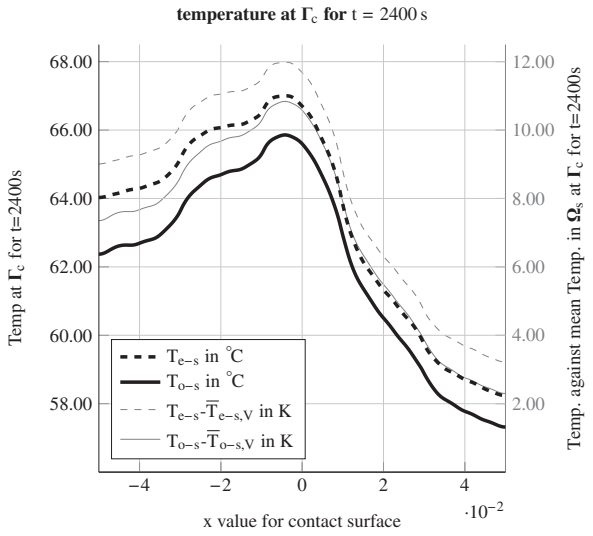

Fig. 8. Temperature plot at the contact surface for $t = t_f$ (e_s="equally spaced", o_s="optimal spaced").

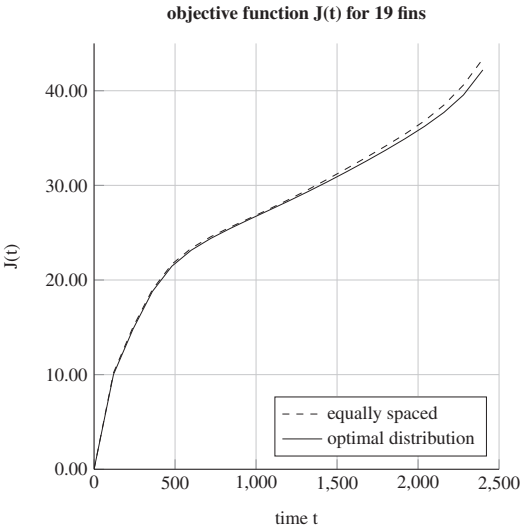

Fig. 9. Objective function $J(t)$ for varying times.

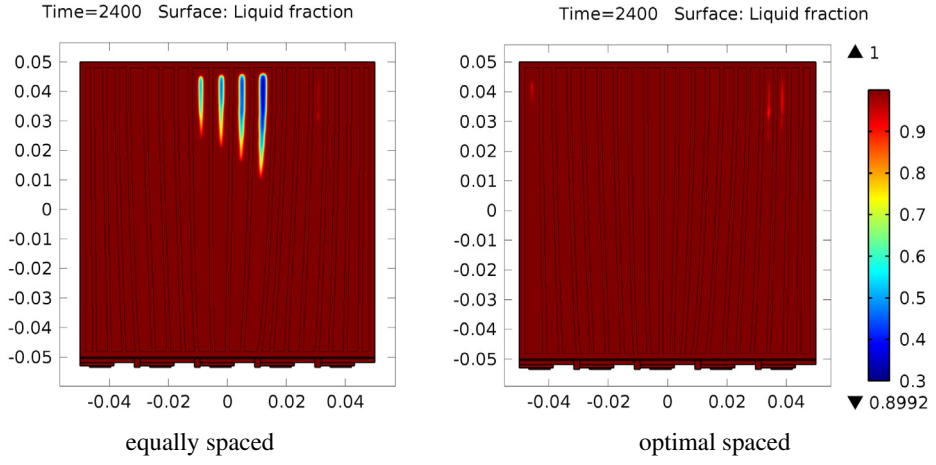

Fig. 7. Liquid fraction of CLHS at $t = 2400$ s.

Table 2
Temperature at the contact surface for $t = t_f$.

x	−0.05	−0.039	−0.028	−0.017	−0.006	0.005	0.016	0.027	0.039	0.05
$T_{e,11} =$	340.89	340.71	338.46	336.84	337.21	335.56	337.18	335.52	338.16	336.53
$T_{o,11} =$	341.46	341.52	338.9	337.31	337.54	336.02	337.48	335.89	338.42	336.94
$T_{e,14} =$	343.12	342.99	340.33	338.84	338.81	337.4	338.73	337.2	339.57	338.09
$T_{o,14} =$	343.93	343.72	341.03	339.67	339.44	338.21	339.3	337.97	340.1	338.68
$T_{e,17} =$	345.38	344.79	342.31	340.74	340.43	339.32	340.13	338.97	340.91	339.8
$T_{o,17} =$	344.16	343.51	341.04	339.52	339.1	338.16	338.77	337.7	339.55	338.46
$T_{e,19} =$	340.16	339.89	337.12	336.01	335.31	334.79	335.05	334.26	335.95	334.89
$T_{o,19} =$	338.4	337.99	335.42	334.28	333.59	333.12	333.41	332.52	334.4	333.1
$T_{e,23} =$	336.66	336.4	333.79	332.76	332.08	331.68	331.95	331.02	333.04	331.52
$T_{o,23} =$	335.85	335.63	333.11	332.07	331.49	331.15	331.39	330.47	332.54	331.02

Table 3
Optimal parameter sets and equal parameter sets (values are multiplied by 100).

	x_1	x_2	x_3	x_4	x_5	x_6	x_7	x_8	x_9	x_{10}	x_{11}	x_{12}	x_{13}
11_o	−3.49	−2.51	−1.55	−0.88	−0.23	0.34	0.96	1.94	2.7	3.53	4.29		
11_e	−4.17	−3.33	−2.5	−1.67	−0.83	0	0.83	1.67	2.5	3.33	4.17		
14_o	−3.95	−3.14	−2.53	−1.88	−1.17	−0.6	−0.07	0.4	0.85	1.56	2.27	2.86	3.48
14_e	−4.33	−3.67	−3	−2.33	−1.67	−1	−0.33	0.33	1	1.67	2.33	3	3.67
17_o	−4.08	−3.31	−2.71	−2.15	−1.6	−0.99	−0.56	−0.1	0.29	0.73	1.27	1.92	2.47
17_e	−4.44	−3.89	−3.33	−2.78	−2.22	−1.67	−1.11	−0.56	0	0.56	1.11	1.67	2.22
19_o	−4.13	−3.61	−2.96	−2.55	−2.04	−1.52	−1.03	−0.62	−0.21	0.15	0.52	0.84	1.34
19_e	−4.5	−4	−3.5	−3	−2.5	−2	−1.5	−1	−0.5	0	.5	1	1.5
23_o	−4.45	−3.67	−3.19	−3.18	−2.77	−2.13	−1.73	−1.72	−1.4	−0.97	−0.96	−0.45	0
23_e	−4.58	−4.17	−3.75	−3.33	−2.92	−2.5	−2.08	−1.67	−1.25	−0.83	−0.42	0	0.42

	x_{14}	x_{15}	x_{16}	x_{17}	x_{18}	x_{19}	x_{20}	x_{21}	x_{22}	x_{23}
14_o	4.14									
14_e	4.33									
17_o	2.93	3.53	3.87	4.46						
17_e	2.78	3.33	3.89	4.44						
19_o	1.92	2.38	2.84	3.39	3.95	4.42				
19_e	2	2.5	3	3.5	4	4.5				
23_o	0.44	0.78	1.31	1.86	2.45	2.83	3.54	3.77	4.28	4.29
23_e	0.83	1.25	1.67	2.08	2.5	2.92	3.33	3.75	4.17	4.58

6. Summary

In this work it has been shown, how an arbitrary CLHS design can be simulated and how this model can be used for optimization programs. Furthermore it has been shown, that an optimization of the distribution of fins inside a CLHS for non-uniform heat loads will lead to an improved design and might be beneficial in the development of CLHS-systems. Optimal results were up to 2 K better than an equally distributed fin CLHS for a certain aluminum/PCM-ratio. It could be observed that the fins should be condensed around the higher head loads.

The constructed CLHS consists of fins, which are aligned to the gradient of the time averaged temperature-field without any fins. An algorithm for a calculation of an initial population has been shown leading to highly diverse populations.

References

[1] E. Lohse, G. Schmitz, Performance assessment of regularly structured composite latent heat storages for temporary cooling of electronic components, Int. J. Refrig. 35 (4) (2012) 1145–1155, http://dx.doi.org/10.1016/j.ijrefrig.2011.12.011. ISSN 0140-7007.

[2] R. Padovan, M. Manzan, Genetic optimization of a PCM enhanced storage tank for solar domestic hot water systems, Solar Energy 103 (0) (2014) 563–573, http://dx.doi.org/10.1016/j.solener.2013.12.034. ISSN 0038-092X.

[3] P.P. Levin, A. Shitzer, G. Hetsroni, Numerical optimization of a PCM-based heat sink with internal fins, Int. J. Heat Mass Transfer 61 (0) (2013) 638–645, http://dx.doi.org/10.1016/j.ijheatmasstransfer.2013.01.056. ISSN 0017-9310.

[4] Atul Nagose, Ankit Somani, Aviral Shrot, Arunn Narasimha, Genetic algorithm based optimization of PCM based heat sinks and effect of heat sink parameters on operational time, J. Heat Transfer 130 (2008). ISSN 0022-1481.

[5] R. Baby, C. Balaji, Experimental investigations on phase change material based finned heat sinks for electronic equipment cooling, Int. J. Heat Mass Transfer 55 (5–6) (2012) 1642–1649, http://dx.doi.org/10.1016/j.ijheatmasstransfer.2011.11.020. ISSN 0017-9310.

[6] R. Baby, C. Balaji, Thermal optimization of PCM based pin fin heat sinks: an experimental study, Appl. Therm. Eng. 54 (1) (2013) 65–77, http://dx.doi.org/10.1016/j.applthermaleng.2012.10.056. ISSN 1359-4311.

[7] E. Lohse, Design of regularly structured composite latent heat storages for thermal management applications (Ph.D. thesis), Technische Universität Hamburg Harburg, 2013.

[8] V. Srinivas, G. Ananthasuresh, Analysis and topology optimization of heat sinks with a phase-change material on COMSOL multiphysics platform, in: COMSOL Users Conference 1. Bangalore, 2006.